

Structural, elastic, and electronic properties of newly discovered Li_2PtSi_3 superconductor: Effect of transition metals

M. A. Alam¹, M. A. Hadi², M. T. Nasir², M. Roknuzzaman³, F. Parvin², M. A. K. Zilani¹, A. K. M. A. Islam^{2,4} and S. H. Naqib^{2*}

¹Department of Physics, Rajshahi University of Engineering and Technology, Rajshahi-6204, Bangladesh

²Department of Physics, University of Rajshahi, Rajshahi-6205, Bangladesh

³Department of Physics, Jessore University of Science and Technology, Jessore-7408, Bangladesh

⁴International Islamic University Chittagong, 154/A College road, Chittagong, Bangladesh

Abstract

First-principles calculations within the density functional theory (DFT) with GGA-PBE exchange-correlation scheme have been employed to predict the structural, the elastic and the electronic properties of newly discovered lithium silicide superconductor, Li_2PtSi_3 , for the first time. All the theoretical results are compared with those calculated recently for isostructural Li_2IrSi_3 . The present study sheds light on the effect of replacement of transition metal element Ir with Pt on different mechanical, electronic, and superconducting properties. The effect of spin-orbit coupling on electronic band structure was found to be insignificant for Li_2PtSi_3 . The difference in superconducting transition temperatures of Li_2PtSi_3 and Li_2IrSi_3 arises primarily due to the difference in electronic energy density of states at the Fermi level. Somewhat reduced Debye temperature in Li_2PtSi_3 plays a minor role. We have discussed the implications of the theoretical results in details in this study.

Keywords: Silicide superconductors; Structural parameters; Elastic properties; Electronic structures

1. Introduction

Because of comparable electronegativity with silicon, transition metals tend to form strong covalent bond with it. In realizing phonon-mediated superconductivity with a high T_c , the covalent character of atomic bonding can play an important role. Transition metal silicides were identified as superconductors at the middle of 20th century. V_3Si has been the best example for early silicide superconductor with $T_c = 17$ K [1]. The possibility of tuning the chemical potential (Fermi energy, in practice) due to different transition metals can, in theory, provide with a way to synthesize new silicide superconductors with significantly higher T_c . Due to this reason, superconductivity in metallic silicides has drawn noticeable attention. Hirai and coworkers reported about the synthesis of silicide superconductors Li_2IrSi_3 , Li_2PtSi_3 , and Li_2RhSi_3 in a recent publication [2]. Among these newly synthesized materials, Li_2IrSi_3 has a T_c of 3.7 K, highest among the three. Li_2IrSi_3 crystallizes in the hexagonal structure with space group $P6_3/mmc$ (No. 194). The crystal structure is composed of Si triangles connected by Ir atoms, resulting in a three-dimensional network of covalent bonds. The antiprisms, IrSi_6 stacking along the c -axis, are connected by Si triangles. Li_2PtSi_3 and Li_2RhSi_3 are isostructural with Li_2IrSi_3 . Theoretical studies of various physical properties of Li_2IrSi_3 have been carried out recently [3, 4] but no theoretical work has been done on Li_2PtSi_3 and Li_2RhSi_3 till date. This motivates us to study theoretically the effect of transition metal replacement in silicide superconductors. In this paper, the structural, elastic and electronic properties of Li_2PtSi_3 have been explored using the first-principles calculations and compared with Li_2IrSi_3 . Replacing Ir with Pt affects all the properties under study. We have discussed these in the subsequent sections.

The rest of the paper has been organized as follows: In Section 2, a short description of the computational methods employed here has been presented. The results are presented and discussed in Section 3. Section 4 consists of a brief summary of the findings and conclusions.

2. Computational Procedures

We have used hexagonal $P6_3/mmc$ (space group No. 194), to determine the structural parameters of Li_2PtSi_3 via geometry optimization. The first-principles calculations were performed by using the Cambridge Serial Total Energy Package (CASTEP) code [5], which is based on the widely employed

* Corresponding author: salehnaqib@yahoo.com

density functional theory (DFT) [6, 7] within the plane-wave pseudopotential approach. The Kohn-Sham equations were solved using the Perdew-Burke-Ernzerhof generalized gradient approximation (PBE-GGA) [8] for the exchange-correlation. Vanderbilt-type ultrasoft pseudopotentials [9] were applied to model the electron-ion interactions. Throughout the calculations, a plane-wave cutoff energy of 500 eV was chosen to determine the number of plane waves in the expansion. The crystal structures were fully relaxed by the Broyden-Fletcher-Goldfrab-Shanno (BFGS) optimization algorithm [10]. Special k -points sampling integration over the Brillouin zone was performed by using the Monkhorst-Pack method [11] with a $11 \times 11 \times 6$ mesh. The tolerance of the various parameters are as follows – the energy tolerance used in the ab-initio calculations is 5×10^{-7} eV/atom, the magnitude of change in total energy is 5×10^{-6} eV/atom, the maximum force is 0.01 eV/Å, the maximum stress is 0.02 GPa, and that for the maximum atomic displacement is 5×10^{-4} Å. Spin-orbit coupling (SOC) was also incorporated for electronic band structure calculations and geometry optimization. For the silicide under study, SOC does not have a significant effect on various physical properties.

CASTEP calculates the elastic properties from the first-principles using the finite strain theory [12], which gives the elastic constants as the proportionality coefficients relating the theoretical strain (ϵ_i) to the computed stress, $\sigma_i = C_{ij} \epsilon_j$. From the values of C_{ij} , the polycrystalline bulk modulus B and shear modulus G can be evaluated using the Voigt-Reuss-Hill approximation [13-15]. In addition, the Young's modulus Y , Poisson's ratio ν , and shear anisotropy factor A , can be estimated using the equations $Y = (9GB)/(3B + G)$, $\nu = (3B - 2G)/(6B + 2G)$ and $A = 4C_{44}/(C_{11} + C_{33} - 2C_{13})$, respectively. The Debye temperature, θ_D , is determined from the following equations [16]: $\theta_D = h/k_B [3n/(4\pi V)]^{1/3} v_m$, with $v_m = [1/3(1/v_l^3 + 2/v_t^3)]^{-1/3}$, $v_l = [(3B + 4G)/3\rho]^{1/2}$, and $v_t = [G/\rho]^{1/2}$. Here, v_l and v_t are the longitudinal and transverse sound velocities which determine the average sound velocity, v_m , in crystalline solids. V is the unit cell volume and n being the number of atoms within a unit cell.

The theoretical estimates of Vickers' hardness for crystals with metallic bonding is evaluated from the well established empirical formula [17, 18]: $H_V = [\prod (H_v^\mu)^{n^\mu}]^{1/\sum n^\mu}$, with the individual bond hardness given by, $H_v^\mu = 740(P^\mu - P^{\mu'}) (v_b^\mu)^{-5/3}$. Here P^μ is the Mulliken population of the μ -type bond, $P^\mu = n_{free}^\mu / V$ is the metallic population, and v_b^μ is the volume of μ -type bond.

It should be noted that the elastic properties are closely related to the crystal structure and the nature of bonding among the ions within a compound. These factors, in turn, determine the phonon spectrum and the Debye temperature. Therefore, elastic constants are not only the primary parameters for the understanding of mechanical properties; they have relevance to the phenomenon of superconductivity in superconducting compounds as well.

3. Results and discussion

3.1. Structural properties

The ground state structure of Li_2PtSi_3 optimized with respect to lattice constants and internal atomic positions in the present investigation is shown in Figure.1. The unit cell contains two formula units consisting of 12 atoms. The optimized Li atoms are situated at the $4f$ Wyckoff site with fractional coordinates (1/3, 2/3, 0.5663). The Si atoms occupy the $6h$ Wyckoff position with fractional coordinates (0.3527, 0.17634, 3/4). The Pt atoms are positioned at the $2a$ Wyckoff site with fractional coordinates (0, 0, 0). The calculated results for the structural properties of Li_2PtSi_3 are presented in Table 1 along with the available data for the isostructural Li_2IrSi_3 . It can be seen from Table 1 that the replacement of Ir with Pt affects the lattice constants, unit cell volume, and bulk modulus. The lattice constants a and c increase by 1.30% and 0.25%, respectively, whereas, the unit cell volume V , increases by 2.87% compared to the experimental value of that of Li_2IrSi_3 [2]. The bulk modulus B decreases significantly, by 8.40%, with respect to the theoretical result of Li_2IrSi_3 [4].

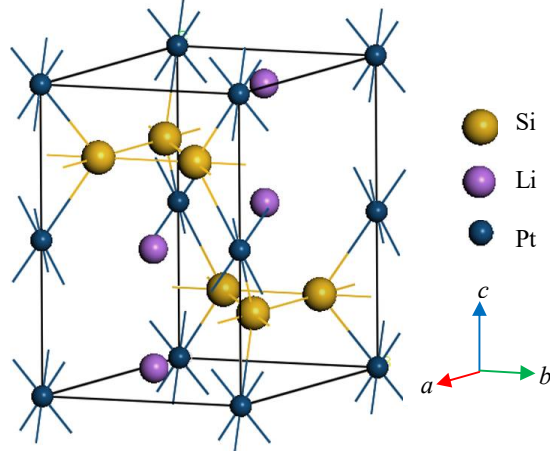


Fig. 1. The unit cell of hexagonal silicide superconductor Li_2PtSi_3 .

Table 1. Lattice constants a and c (in \AA), internal parameter z_{Li} , hexagonal ratio c/a , unit cell volume V (in \AA^3), and bulk modulus B (GPa) with its pressure derivative B' for hexagonal Li_2PtSi_3 .

Compounds	A	c	c/a	z_{Li}	V	B	B'	Remarks
Li_2PtSi_3	5.0826	7.8600	1.5465	0.5663	175.84	106.16	4.50	This study
Li_2IrSi_3	5.0176	7.8402	1.5625	0.5604	170.94			Expt. [2]
	5.0069	7.8655	1.5709	0.5589	170.76	115.90	4.24	Calc. [4]
	5.0183	7.8414	1.5626		170.42			Calc. [3]

3.2. Elastic properties

Calculated elastic coefficients of Li_2PtSi_3 are listed in Table 2 along with the previously calculated values for isostructural Li_2IrSi_3 [4]. The positive values of C_{11} , C_{44} , $(C_{11} - C_{12})$, and $\{(C_{11} + C_{12})C_{33} - 2C_{12}^2\}$ conform with the Born mechanical stability criteria [19] for Li_2PtSi_3 . The small values of C_{12} and C_{13} suggest that Li_2PtSi_3 should be classified as a brittle material [20]. The widely used Pugh's criterion [21] and the Frantsevich's rule [22] also favor this classification. Pugh's criterion suggests that a material will be brittle if its $G/B > 0.5$, otherwise it is ductile. The Frantsevich's rule states that the mechanical property of a material will be dominated with brittleness when Poisson's ratio $\nu < 0.33$; if $\nu > 0.33$, the mechanical property of the material mainly exhibits ductile nature. As can be seen from Table 2, the newly synthesized Li_2PtSi_3 should be brittle in nature like Li_2IrSi_3 . Qualitatively, substitution of Ir with Pt reduces the brittleness of these compounds. In fact, Li_2PtSi_3 lies at the borderline between ductility and brittleness. The comparatively high value of Poisson's ratio indicates that the directional covalent bonding in Li_2PtSi_3 is not as strong as in Li_2IrSi_3 .

The difference between C_{11} and C_{33} indicates about the elastic anisotropy possessed by the crystal. Elastic anisotropy results from different types of bonding in different directions. Inherently, majority of the known crystals are elastically anisotropic, and an accurate description of such anisotropic behavior has a significant implication in engineering, applied science, and crystal physics, since it correlates with the possibility of appearance of micro-cracks inside the crystals under stress. It is seen that the difference between C_{11} and C_{33} reduces when Ir is substituted by Pt. Therefore, the elastic anisotropy in Li_2PtSi_3 should be low in comparison with Li_2IrSi_3 . We have also estimated the shear anisotropy factor, given by $A = 4C_{44}/(C_{11} + C_{33} - 2C_{13})$. For an isotropic crystal, $A = 1$, and the deviation from unity measures the degree of elastic anisotropy. The calculated results show that the phase Li_2PtSi_3 is almost isotropic, whereas Li_2IrSi_3 possesses small anisotropy for the shear plane $\{100\}$ between the directions $\langle 011 \rangle$ and $\langle 010 \rangle$. Yet, another anisotropy parameter can be obtained from the ratio between the uniaxial compressions along the c - and a -axis for a hexagonal crystal: k_c/k_a

$= (C_{11} + C_{12} - 2C_{13})/(C_{33} - C_{13})$. The deviation from unity for Li_2PtSi_3 is small in comparison with Li_2IrSi_3 and it lacks elastic anisotropy [23].

The ratio between the bulk modulus B and elastic constant C_{44} may be interpreted as a gauge of plasticity [24]. The plasticity can also be estimated from the value of $(C_{11} - C_{12})$ and the Young's modulus Y [25]. The smaller values of $(C_{11} - C_{12})$ and Y indicate better plasticity of Li_2PtSi_3 in comparison with Li_2IrSi_3 . Furthermore, B/C_{44} ratio measures the lubricity which gives the index of machinability of bulk materials. The values of this ratio signify that the degree of lubricity and machinability of Li_2PtSi_3 is almost similar to Li_2IrSi_3 . Bulk and shear moduli are considered as an important parameter for estimating the hardness of bulk materials. The small values of these two parameters for Li_2IrSi_3 and Li_2PtSi_3 imply that they may be grouped into high compressible materials. Again, in comparison to Li_2IrSi_3 , Li_2PtSi_3 is more compressible. Young's modulus gives a measure of stiffness and it is seen that substitution of Pt in place of Ir makes the compound less stiff (Table 2). Therefore, Pt causes a significant reduction of the independent elastic constants (C_{11} , C_{33} , and C_{44}) and all the elastic moduli (B , G , and Y). At the same time, this substitution results in a lowering of the brittleness, elastic anisotropy, and strength of the directional covalent bonding in Li_2PtSi_3 .

Table 2. Single crystal elastic constants C_{ij} (GPa), polycrystalline bulk modulus B (GPa), shear modulus G (GPa), Young modulus Y (GPa), Pugh's ratio G/B , Poisson's ratio ν , and anisotropy factor A and k_c/k_a of Li_2PtSi_3 and Li_2IrSi_3 .

Compounds	Single crystal elastic constants					Polycrystalline elastic properties							Remarks
	C_{11}	C_{12}	C_{13}	C_{33}	C_{44}	B	G	Y	G/B	ν	A	k_c/k_a	
Li_2PtSi_3	160	82	63	224	67	106	55	141	0.52	0.28	1.04	0.72	This study
Li_2IrSi_3	198	71	55	295	68	116	72	179	0.62	0.24	0.71	0.66	Calc. [4]

The Debye temperature, calculated from longitudinal, transverse, and average sound velocities within the present formalism is listed in Table 3. It is observed that the replacement of Ir with Pt results in an appreciable reduction in the Debye temperature. It is known that the Debye temperature is indicative of the strength of covalent bonding in a crystal. Therefore, we may conclude again that the covalent bonding in Li_2PtSi_3 is weaker than that of Li_2IrSi_3 .

Table 3. Calculated density (ρ in gm/cm^3), longitudinal, transverse, and average sound velocities (v_l , v_t , and v_m in km/s) and Debye temperature (θ_D in K).

Compounds	ρ	v_l	v_t	v_m	θ_D
Li_2PtSi_3	5.538	5.691	3.151	3.510	427
Li_2IrSi_3	5.641	6.130	3.573	3.963	488 [4], 486 ^a , 488 ^b

^aRef. [2]^{Expt.}

^bRef. [3]^{Calc.}

3.3. Electronic and bonding properties

In Fig. 2a, the energy band, without SOC, of Li_2PtSi_3 with optimized lattice parameters along the high symmetry directions within the first Brillouin zone is presented. The Fermi level lies just below the lowest conduction band near the Γ point. The occupied valence bands spread from -12.8 eV to the Fermi level E_F , and few of them just crosses the Fermi level along the M-L direction. Further, two of valence bands overlap with the conduction band near the M point. Consequently, no band gap is seen and the compound behaves as a metallic system like the isostructural Li_2IrSi_3 . The gross features of the band structures of Li_2PtSi_3 and Li_2IrSi_3 are almost similar.

The total and partial energy density of states (DOS) of Li_2PtSi_3 is shown in Fig. 2b. The total DOS has a finite value at the Fermi level $N(E_F)$, around 1.48 states per eV per unit cell, which is small in comparison with the values found in literatures for Li_2IrSi_3 [2-4] (~ 3.5 states per eV per unit cell). The DOS at the Fermi level reduces significantly due to the replacement of Ir by Pt. Since the electron phonon coupling constant, λ , varies linearly with $N(E_F)$, a lower value of electronic density of states at

the Fermi level implies a lower value of T_c , given that the matrix element of electron-phonon interaction is fixed. This provides us with an explanation for the reduced value of $T_c = 1.8$ K for Li_2PtSi_3 in comparison to that for Li_2IrSi_3 , where $T_c = 3.7$ K.

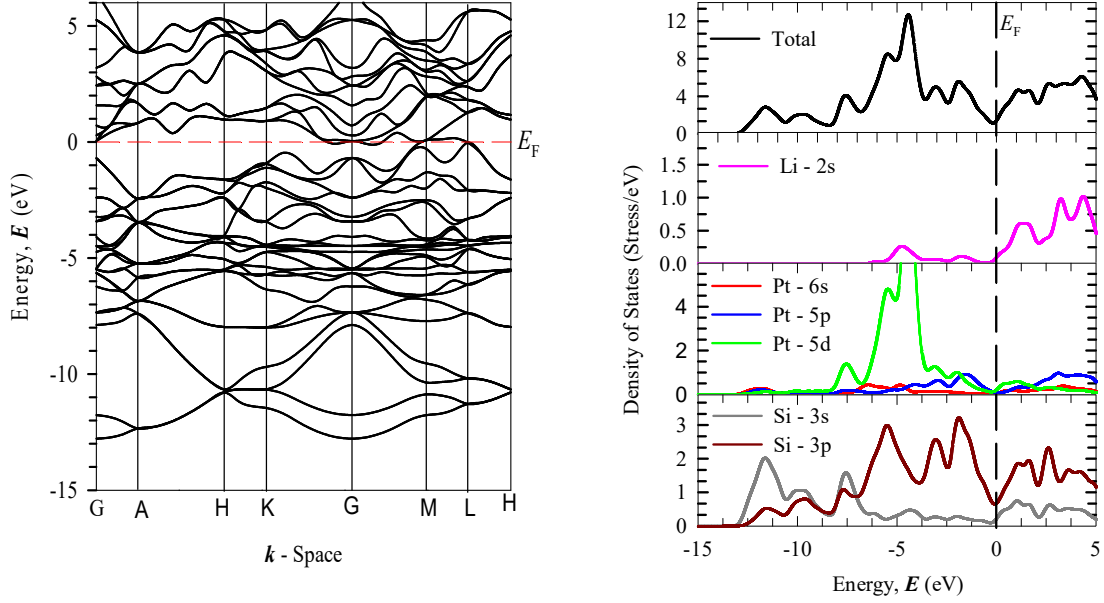


Fig. 2. Electronic structure of Li_2PtSi_3 : (a) Band structure at equilibrium lattice parameters along the high symmetry directions within the Brillouin zone and (b) Total and partial energy density of states. The Fermi level is set to 0 eV.

The details of the peak structures and the relative heights in the total and partial DOSs for Li_2PtSi_3 are roughly similar to those found for Li_2IrSi_3 [3, 4]. One notable difference is that the DOS at the Fermi level for Li_2PtSi_3 is situated at a dip and a pseudogap appeared at the left of the Fermi level, whereas the DOS at the Fermi level for Li_2IrSi_3 lies just below a peak structure.

Inspection of the partial DOSs reveals that the DOS at the Fermi level originates mainly from Pt $5d$ and Si $3p$ states. This is due to the d -resonance in the vicinity at the Fermi level, similar to the case for Li_2IrSi_3 where the d electrons of the Ir atoms play a similar role. The lowest-lying valence bands of both these silicide superconductors with two peak structures consisting of $3s$ and $3p$ states of Si occupy almost same energy range. But this band for Li_2PtSi_3 is not as wide as Li_2IrSi_3 [4]. The covalent Si–Si bond that forms a three dimensional rigid network as a whole in case of Li_2IrSi_3 [2] is stronger than that of Li_2PtSi_3 . The rest of the valence band arises mainly from the strong hybridization of $3s$ and $3p$ states of silicon with $5d$ states of transition metal Pt in Li_2PtSi_3 or Ir in Li_2IrSi_3 .

Table 4. Atomic population analysis of Li_2PtSi_3 and Li_2IrSi_3 .

Compounds	Species	Mulliken Atomic populations				Charge (e)	Effective valence Charge (e)
		<i>s</i>	<i>p</i>	<i>D</i>	Total		
Li_2PtSi_3	Li	1.90	0.00	0.00	1.90	1.10	1.90
	Pt	0.91	1.62	9.02	11.54	−1.54	3.54
	Si	1.36	2.86	0.00	4.22	−0.22	
Li_2IrSi_3	Li	1.99	0.00	0.00	1.99	1.01	1.99
	Ir	0.77	1.31	8.26	10.33	−1.33	5.33
	Si	1.37	2.86	0.00	4.23	−0.23	

Table 5. Calculated Mulliken bond number n^μ , bond length d^μ , bond overlap population P^μ , bond volume v_b^μ and bond hardness H_v^μ of μ -type bond and metallic population $P^{\mu'}$ and Vickers hardness H_v of Li_2PtSi_3 and Li_2IrSi_3

Compounds	Bond	n^μ	d^μ (Å)	P^μ	$P^{\mu'}$	v_b^μ (Å ³)	H_v^μ (GPa)	H_v (GPa)
Li_2PtSi_3	Si–Si	6	2.39337	0.51	0.00125	7.55875	12.93162	5.87
	Si–Pt	12	2.50435	0.26	0.00125	8.65975	5.24429	
Li_2IrSi_3	Si–Si	6	2.43154	0.56	0.03573	9.22726	9.55723	6.21
	Si–Ir	12	2.46525	0.33	0.03573	9.61637	5.00756	

To explore the bonding nature of newly synthesized silicide superconductors Li_2PtSi_3 and Li_2IrSi_3 , the Mulliken atomic populations are calculated for the first time. The atomic populations are listed in Table 4 along with the effective valence. The difference between the formal ionic charge and the Mulliken charge on the anion species in the crystal is defined as the effective valence that identifies a bond either as covalent or ionic. An ideal ionic bond occurs when the effective valence is exactly zero. The strength of the covalent bond increases if the effective valence shows an increasing tendency towards positive values. The last column of Table 4 represents the calculated effective valence that indicates significant covalent bonding in both the silicides. Table 5 lists the bond overlap populations for the Si–Si and Si–Pt bonds of Li_2PtSi_3 and Si–Si and Si–Ir bonds of Li_2IrSi_3 . A value of the overlap population close to zero implies that the interaction between the electronic populations of the two atoms is negligible. A low overlap population also indicates a high degree of ionicity, whereas a high value implies a high degree of covalency in the chemical bond. Therefore, it follows from Table 5 that Si–Si bond is more covalent in Li_2IrSi_3 than that in Li_2PtSi_3 .

The degree of metallicity may be calculated from the parameter $f_m = P^{\mu'}/P^\mu$ [16, 26]. The calculated metallicity of the Si–Si and Si–Pt bonds in Li_2PtSi_3 are 0.00245 and 0.00481, respectively. For Li_2IrSi_3 , the calculated metallicity for Si–Si and Si–Ir bonds are 0.06380 and 0.10827, respectively, suggesting that the Si–Ir bond has strong metallic characteristics. Table 5 shows that the bonding nature in the two new silicide superconductors may be described as a combination of covalent and metallic. Table 5 also lists the calculated Vickers hardness that reflects the crystal structure and chemical bonding of the compounds. The total Vickers hardness is obtained by calculating the geometrical average of the individual bond hardness of the compound. The general relationship between the bond-length and hardness is such that the hardness increases with decreasing the bond-length. Considering this relationship, the Si–Si bonds are expected to be harder than other bonds. The calculated values of the Vickers hardness for Li_2PtSi_3 and Li_2IrSi_3 are found to be 5.87 and 6.21 GPa, respectively. It is evident that the Vickers hardness reduces when Ir is replaced with Pt and therefore, Li_2PtSi_3 is relatively soft and easily mechivable compared to Li_2IrSi_3 .

3. Conclusions

A first-principles study on the structural, elastic, bonding, and the electronic properties of Li_2PtSi_3 is done for the first time. The theoretical results have been compared with those found for isostructural Li_2IrSi_3 to explore the role of Pt in place of Ir. Replacing Ir with Pt affects the lattice parameters, elastic constants, bulk modulus, shear modulus, Young's modulus, Poisson's ratio, Pugh's ratio, elastic anisotropy, Debye temperature, and Vickers hardness to a varying degree. The electronic properties such as band structure, total and partial DOS and Mulliken bond populations are also affected. The most significant change is seen in the drastically reduced electronic density of states at the Fermi level of Li_2PtSi_3 . This should be the primary reason for significantly reduced superconducting T_c in this compound. Using the theoretically estimated Debye temperature and the T_c equation due to Allen-Dynes [27], we have calculated the electron-phonon coupling constant, $\lambda \sim 0.4$, to get the experimental $T_c = 1.8$ K. Therefore, like Li_2IrSi_3 , Li_2PtSi_3 is also a weakly coupled BCS superconductor. It would be interesting to synthesize Li_2ReSi_3 and Li_2OsSi_3 in future. These silicides may exhibit superconductivity at higher temperatures because of $5d^56s^2$ and $5d^66s^2$ electronic configurations, respectively, which may enhance $N(E_F)$. As mentioned earlier, inclusion of SOC does

not change most of the properties in any significant way. The only noticeable effect of SOC is the lifting of degeneracy of the high-energy electronic bands ($\sim 4 - 6$ eV).

References

- [1] Hardy G F and Hulm J K 1953 *Phys. Rev.* **89** 884
- [2] Hirai D, Kawakami R, Magdysyuk O, Dinnebier R E, Yaresko A, and Takagi H 2014 *J. Phys. Soc. Japan* **83** 103703
- [3] Lu H -Y, Yang N -N, Geng L, Chen S, Yang Y, Lu W -J, Wang W -S, and Sun J 2015 *Europhys. Lett.* **110** 17003
- [4] Hadi M A, Alam M A, Roknuzzaman M, Nasir M T, Islam A K M A, and Naqib S H 2015 *Chinese. Physics B* **24** 117401
- [5] Clark S J, Segall M D, Pickard C J, Hasnip P J, Probert M I J, *Zeitschrift für Kristallographie* **220** 567
- [6] Hohenberg P and Kohn W 1964 *Phys. Rev.* **136** B864
- [7] Kohn W and Sham L J 1965 *Phys. Rev.* **140** A1133
- [8] Perdew J P, Burke K, and Ernzerhof M 1996 *Phys. Rev. Lett.* **77** 3865
- [9] Vanderbilt D 1990 *Phys. Rev. B* **41** 7892
- [10] Fischer T H and Almlöf J 1992 *J. Phys. Chem.* **96** 9768
- [11] Monkhorst H J, Pack J D 1976 *Phys. Rev. B* **13** 5188
- [12] Murnaghan F D 1951 *Finite Deformation of an Elastic Solid* (New York: Wiley & Sons)
- [13] Voigt W *Lehrbuch der Kristallphysik* 1928 (Leipzig: Taubner press)
- [14] Reuss A and Angew Z 1929 *Math. Mech.* **9**, 49
- [15] Hill R 1952 *Proc. Phys. Soc. A* **65**, 349
- [16] Anderson O L 1963 *J. Phys. Chem. Solids* **24** 909
- [17] Gao F M 2006 *Physical Review B* **73**, 132104
- [18] Gou H Y, Hou L, Zhang J W, and Gao F M 2008 *Applied Physics Letters* **92**, 241901
- [19] Born M 1940 *Math. Proc. Camb. Philos. Soc.* **36** 160
- [20] Romero M and Escamilla R 2012 *Comp. Mater. Sci.* **55** 142
- [21] Pugh S F 1954 *Philos. Mag.* **45**, 823
- [22] Frantsevich I N, Voronov F F, and Bokuta S A 1983 *Elastic constants and elastic moduli of metals and insulators handbook* (Naukova Dumka, Kiev) pp. 60–180.
- [23] Du Y L, Sun Z M, Hashimoto H, and Barsoum M W 2009 *Phys. Lett. A* **374** 78
- [24] Vitos L, Korzhavyi P A, and Johansson B 2003 *Nature Mater.* **2** 25
- [25] Mattesini M, Ahuja R, and Johansson B 2003 *Phys. Rev. B* **68** 184108
- [26] Hadi M A, Ali M S, Naqib S H, and Islam A K M A 2013 *Int. J. Comp. Mater. Sci. Eng.* **2** 1350007
- [27] Allen P B and Dynes R C 1975 *Phys. Rev. B* **12** 905